DOI: 10.1021/ma101162x

Macromolecules
ARTICLE

Form II Poly(3-butylthiophene): Crystal Structure and Preferred Orientation in Spherulitic Thin Films

Annamaria Buono,[†] Nguyen Hoai Son,[†] Guido Raos,[†] Liliana Gila,[§] Alessandra Cominetti,[§] Marinella Catellani,[‡] and Stefano Valdo Meille*,[†]

[†]*Dipartimento di Chimica, Materiali ed Ingegneria Chimica "Giulio Natta" del Politecnico di Milano, via Mancinelli 7, I-20131 Milano, Italy,* [‡]*CNR, Istituto per lo Studio delle Macromolecole (ISMAC), via Bassini 15, I-20133 Milano, Italy, and* [§]*Istituto Donegani, ENI S.p.A., Via Fauser, 4, 28100 Novara, Italy*

Received May 26, 2010; Revised Manuscript Received July 2, 2010

ABSTRACT: Poly(3-*n*-butylthiophene) (P3BT) samples with different average molecular weights and head-to-tail regioregularity were crystallized in the form II crystal polymorph either from solution or by annealing with CS_2 vapors. With a combined approach, making also use of literature electron diffraction data, we show that form II is well described by a limit-ordered monoclinic model in space group $P2_1/c$ with lattice parameters $a = 10.76(1)$ Å, $b = 7.77(1)$ Å (chain axis), $c = 9.44(1)$ Å, and $\beta = 64.66°$, yielding a calculated density of 1.29 g/cm^3 in qualitative agreement with proposals by Winokur et al. for the form II structures of regioregular poly(3-octylthiophene) and poly(3-dodecylthiophene) (P3DDT). Our structural model was refined by Rietveld analysis and has been confirmed by molecular mechanics (MM) and molecular dynamics (MD) calculations adopting a thiophene-specific force field developed in our group. Consistent with its higher density and with thermal data, form II shows lower potential energy than the form I′ crystalline polymorph of P3BT. Both the main-chain and the side-chain conformations closely correspond to those found in form I′ polymorph. The form II P3BT refined structural model presents an antidirectional looser stacking and tightly interdigitated layering, different from those observed in the form I family of poly(3-alkythiophenes) (P3ATs) and crystallite dimension of 20−30 Å along the chain axis. This feature and the lamellar structure implied by the spherulitic morphology are consistent with substantial chain-folding for high molecular weight samples. Oriented X-ray diffraction patterns from thin films of form II P3BT are explained assuming that the stacking axis **c**, corresponding to the radial, fast growth direction of the bidimensional form II spherulites, is preferentially in the plane of the film, while the layer axis **a** and the chain axis **b** approach random orientation around **c**, at variance with recent literature suggestions. The small crystal dimensions along the chain axis, the looser stacking, the relevance of chain folding and the spherulitic morphology implying film discontinuity suggest that the form II structural family of P3AT's are less viable than the form I polymorphs for molecular electronics applications.

Introduction

It is well established that the features of hierarchical structural organization in organic semiconductors profoundly affect performance in electronic devices.[1−5] In other words, for a molecular understanding[6−8] of the structure-properties relationship in conjugated polymer solar cells,[1,2,9] field-effect transistors,[4,10] and LEDs,[11] detailed models of the polymer chain organization in crystals, in partially ordered mesophases and at interphases are required but still scarce and largely qualitative. Such considerations apply specifically to the poly(3-alkythiophene) (P3AT) family[2,4,9,12] and to other conjugated polymers families which tend crystallize with difficulty.

Regioregular poly(3-butylthiophene) (P3BT) with adequate morphology has been proved recently to be among the best donor materials, along with poly(3-hexylthiophene) (P3HT), for the assembly of organic solar cells.[13] It is structurally the simplest member of P3AT family maintaining significant degrees of processability and solubility in common organic solvents. It has also been demonstrated that P3BT films are unique among polythiophenes in adopting clear spherulitic morphologies upon controlled treatment with carbon disulfide.[14] These structures have been shown to consist of lamellae of the form II crystalline polymorph of P3BT, evidencing once again the strict correlation between crystalline structure and morphology. Form II is a relatively rare polymorph occurring in a number of regioregular poly(3-alkylthiophenes) (P3AT's),[15−18] especially when low-molecular weight fractions are crystallized from solution. In the case of P3BT, the morphological observations of form II spherulitic structures were complemented by electron diffraction patterns,[14] which are among the very few showing single crystal features[19] in the case of P3AT's. It has been suggested that, in spherulitic films of P3BT, crystals are oriented preferentially so that the chain axis is mainly orthogonal to the film,[14] at variance with what observed in form I where the chain axis lies preferentially in the plane of the film.[4,17] It is surprising that evidence of the form II polymorph in the case of P3HT are scarce in the literature and clear evidence of its occurrence are limited to very low molecular weight fractions.[18]

Along with our fundamental interest[17,20] in P3AT polymorphism,[19,21−23] and more specifically in P3BT polymorphism,[24] it is the apparently unique crystallization behavior of the form II polymorph of P3BT and its potential in achieving new morphologies with a unique main chain orientation with respect to the substrate,[14] that has prompted us to investigate in detail the crystal structure of form II P3BT and its relationship to proposed models of this structural family for other P3ATs.[15,16] In the present paper we devised *limit-ordered*[25] models of the crystal

*Corresponding author. E-mail: valdo.meille@polimi.it.

 Published on Web 07/22/2010

structure, imposing the appropriate chain symmetry and crystallographic equivalence of monomeric units, thus keeping the independent structural parameters at a minimum. The models thus obtained are amenable to investigation by molecular mechanics (MM) and molecular dynamics (MD), for which we used the specific force field developed and optimized in our group,[26] aiming at accurately and consistently account for both intramolecular features (torsion potentials of the π-conjugated backbone and side chains) and intermolecular interactions (van der Waals and electrostatics).

The structural characterization of form II P3BT was carried out using experimental data obtained from three well characterized P3BT samples, allowing to investigate correlations between molecular and morphological features. With a well-defined crystallographic model available we were also able to define the preferred orientation of form II crystallites and of the poly(3-butylhiophene) main chain in thin films. The structural and morphological features making the form II P3AT modifications less viable than form I type polymorphs in organic electronics may now be understood with greater clarity.

Experimental Section

Samples. Sample S was a regioregular P3BT prepared using the McCullough synthetic route, giving regiocontrol at each coupling step in the polymerization.[27a] This polymer was extracted in a Soxhlet apparatus first with methanol and then with diethyl ether, to separate very low molecular weight fractions. It was then dissolved in boiling chloroform and reprecipitated at 40 °C, to obtain a powder which was dried under vacuum at room temperature. The polymer was the same used in previous studies on form I′,[24] but was completely recharacterized by GPC and NMR for consistency with other samples.

Samples AD and AG were fractions obtained from a polymer purchased from Aldrich (batch 11314CE) with a nominal regioregularity of 90%. Both fractions AD and AG (respectively ~13% and ~40% of the original polymer) were insoluble in hexane and soluble in THF. Fraction AD was soluble in ethyl acetate whereas fraction AG was insoluble in both ethyl acetate and in CH_2Cl_2. All the extraction procedures leading to samples AD and AG were performed using a Soxhlet apparatus.

Essential data pertaining to the three samples are summarized in Table I. Molecular weights were determined by high temperature-gel-permeation chromatography using a Waters (HT-GPC 150C) instrument equipped with four columns set for M_w range 200−1 000 000 and a refractive index detector. The eluent was trichlorobenzene which was kept at 80 °C; the eluent rate was 1 mL/min. The instrument was calibrated with polystyrene standards from M_w 1060 to 210 000. Detailed analysis of the regioregularity of the samples would have to take also terminals into account, especially for low molecular weight samples. Furthermore, regioregularity defects with synthetic routes leading to highly regioregular polyalkylthiophenes[27b,c] are found to concentrate in terminal regions. For the samples analyzed in this paper, limiting our analysis to the crystallizing, nonterminal portions of the molecules, the regioregularity at the dyad level was estimated at about 95% or higher by ^{1}H NMR spectroscopy.

X-ray Diffraction and Confocal Microscopy. In the case of the AD form II sample, minute polymer fragments having mass of ca. 0.1 mg, as obtained drying ethyl acetate solution, were mounted on a glass fiber. Samples AG and S were deposited in the form of thin films from $CHCl_3$ solution on glass slides or on silicon and then exposed to CS_2 vapors in covered Petri dishes, leading to form II crystallization.[14] Film thicknesses were typically about 100−200 nm. X-ray diffraction patterns were then directly recorded in grazing incidence diffraction (GID) mode or the samples were gently scratched from the substrate and inserted in a glass capillary for subsequent measurement. X-ray diffraction patterns of samples in capillaries or mounted on glass fibres, were recorded using graphite monochromated Cu Kα radiation (λ = 1.54178 Å), on a Siemens P4 diffractometer equipped with a HiStar 2D detector. The sample-to-detector distance was about 10 cm. Samples were rotated during data collection around the angles ϕ and χ, or around ϕ at χ = 54.7°, to obtain diffraction patterns approaching random crystallite orientations. One-dimensional diffraction patterns were obtained by integrating 2D spectra over the azimuthal angle χ at constant 2θ, with appropriate geometrical corrections.

Table 1. Native Polymorphism, Molecular Masses, and Chain Length of the Studied P3BT Samples (See Experimental Section)

sample	%	native form	M_n	M_w	DP_W[d]	ECL (Å)[e]
S[a]		I′	9150	18 800	98	370
AD[b]	~11	II	5600	7900	41	160
AG[c]	~44	I′	24 800	44 900	231	880

[a] Methanol and ethyl ether insoluble, $CHCl_3$ soluble fraction of a McCollough type P3BT. [b] Hexane insoluble, soluble in refluxing ethyl acetate or THF. [c] Hexane, ethyl acetate, and CH_2Cl_2 insoluble, soluble in refluxing THF. [d] Degree of polymerization, calculated from M_w, assuming overextimation by ~40% of molecular weights by GPC.[37] [e] Extended chain length (average) estimated from the DP_w value.

Confocal polarized fluorescence images of sample S cast film on glass were collected with a Nikon Eclipse TE2000-U inverted confocal microscope with a long working distance and a Plan Apo VC objective (magnification 60, N.A. 1.4), using an excitation wavelength of 543 nm.

Modeling. Most MM and MD simulations were carried out with the Tinker 4.2 molecular modeling package,[28] using our own force field for oligo- and poly(alkylthiophenes).[26] Accelrys Materials Studio[29] was also employed for visualization and preliminary model selection. Here we only provide a brief overview, as details about the parametrization and testing of the force field are discussed in ref 26e. Bond lengths and angles were assigned standard values by comparison with available crystal structures[30] or ab initio calculations on short oligomers. The most critical parts of the force field are the nonbonded interactions and intramolecular torsion potentials. Lennard-Jones parameters were taken without further adjustments from the OPLS-AA force field.[31] Atomic point charges were obtained by combining the standard OPLS-AA atomic charges and those obtained by fitting the molecular electrostatic potential produced by the ab initio (B3LYP/6-311G**) electron densities of short model oligomers. The torsion potentials for the alkyl side chains were taken directly from the OPLS-AA parametrization for alkanes. The remaining potentials were obtained from ab initio B3LYP/6-311G** calculations on tetrathiophene (torsion about the conjugated backbone) and on 3-ethylthiophene (torsion about the C−C bond connecting the side chain to the backbone).[26]

Results and Discussion

Sample Characterization and Recrystallization in Form II. The main relevant features of the three studied samples are presented in Table 1. Although two of the three samples, are upon isolation in form I′, recrystallization with carbon disulfide[14] of thin films cast from $CHCl_3$ gives rise to well-defined spherulites (see Figure 1) consisting of form II lamellae. The unoriented form II diffraction patterns of the three samples are shown in Figure 2: the pattern due to the crystalline component appears to be very similar, except for minor differences at relatively high angles. Form II P3BT diffraction patterns are clearly identified by the very intense maximum at 2θ = 9.1° corresponding to a an interlayer spacing of about 9.8 Å which distinguishes this polymorph from the form I structural family characterized by a very sharp maximum at 2θ = 6.9−7.0° determined by the characteristic layer spacing of 12.5−13.0 Å.

The maximum at about 2θ = 7.0−7.2° in all three patterns of Figure 2 is broad and rounded as compared to the typical, sharp form I layer maxima. Along with the amorphous

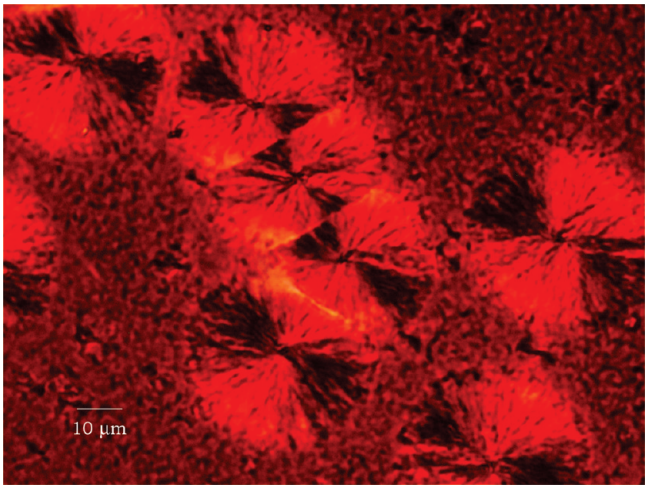

Figure 1. Confocal polarized fluorescence microscopy images of form II P3BT spherulites, resulting from recrystallization of a solution cast sample S film by CS_2 vapors.

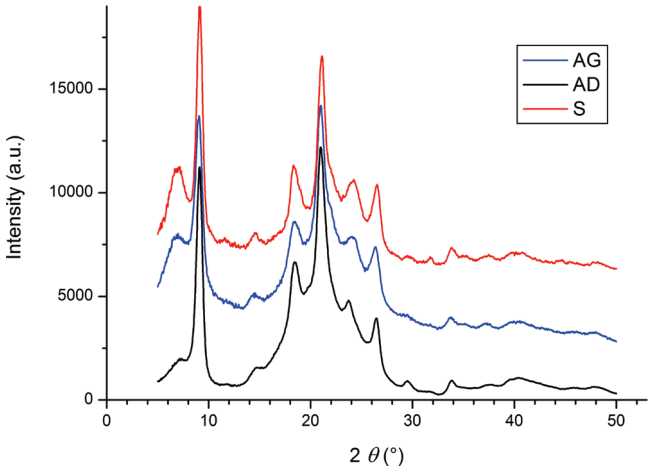

Figure 2. X-ray diffraction patterns of the three different form II P3BT studied: the main structural features of the three samples are reported in Table 1.

background centered around $2\theta \approx 21°$ it shows substantially different relative intensities indicating differences in the non crystalline components of the three samples. The intensity of the peak at $2\theta \approx 7°$ appears to increase roughly with the average molecular weight of the samples and is very low for the lowest molecular weight sample AD.

P3BT Form II Lattices and Molecular and Packing Models. In general, the determination of plausible initial lattice parameters by the analysis of X-ray diffraction patterns of crystalline polymers of the kind reported in Figure 2 and Table 2 is a challenging task. However, from the rectangular bidimensional indexing of electron diffraction (ED) data of the form II of P3BT by Lu et al.,[14] and adopting the standard intrachain periodicity found for form I′ P3BT[24] and other regioregular P3ATs, one may extrapolate an orthorhombic unit cell with a = 9.70 Å, b (chain axis) = 7.78 Å, and c = 9.40 Å. Since the electron diffraction patterns in the literature[14] do not present strict *mm* symmetry, it is also possible to take into consideration alternative, less symmetric lattices. Indeed, the arched diffraction maxima of the ED patterns (see Figures 2 and 4 in ref 10a and Figure 7 in ref 10b) imply polycrystalline rather than single crystalline morphologies. The quasi-orthorhombic symmetry may well result from statistical coexistence of different crystallite

Table 2. Observed Maxima in the X-ray Diffraction Patterns of P3BT, Where Indexing Is Given with Tentative Two-Chain Orthorhombic [a] and Monoclinic [b] Cells

P3BT: Form II			orthorhombic[a]		monoclinic[b]	
$d_{(obs)}$ (Å)	$2\theta_{(obs)}$ (deg)	intensity	*hkl*	$2\theta_{(calc)}$ (deg)	*hkl*	$2\theta_{(calc)}$ (deg)
9.77	9.1	vvs	1 0 0	9.12	1 0 0	9.16
6.05	14.6	w	1 1 0	14.60	1 1 0	14.62
4.88	18.4	m	2 0 0	18.29	2 0 0	18.37
					1 0 2	18.90
4.23	21.0	vs	2 0 1	20.61	0 0 2	20.94
			1 0 2	21.00	2 0 2	21.10
3.70	24.0	m	2 1 2	23.95	2 1 1	23.89
					2 1 2	24.03
3.37	26.5	m	2 0 2	26.41	−1 0 2	26.33
			1 2 1	26.44	3 0 2	26.59
3.0	29.5	w	2 2 0	29.43	2 2 0	29.49
2.85	31.7	vvw	3 1 1	31.44	2 2 2	31.31
					0 0 3	31.64
					3 0 3	31.88
2.65	33.8	w	3 0 2	33.64	−2 0 2	33.59
					0 1 3	33.72
					−3 0 1	33.76
					4 0 2	33.90
					4 0 1	33.95

[a] a = 9.70 Å, b (chain axis) = 7.78 Å, c = 9.40 Å, extrapolated from ref 14, interchanging the b and c axis for consistency with the lattice which proved correct. [b] a = 10.70 Å, b (chain axis) = 7.78 Å, c = 9.40 Å, β = 64.5°.

orientations. A plausible alternative tentative indexing, using a monoclinic cell with a = 10.66 Å, b (chain axis) = 7.78 Å, c = 9.40 Å, and β = 64° can therefore be taken into consideration (Figure 3).

Data concerning the observed X-ray diffraction maxima are reported in Table 2 with the indexing and the related d-spacings calculated according to the mentioned tentative orthorhombic lattice and the monoclinic lattice that was eventually adopted. The monoclinic lattice shows remarkable similarities with the unit cells proposed by Winokur et al.,[15] with respect to both the stacking axis of 9.40 Å and to the monoclinic angle: 64.5° as opposed to 72° found for poly(3-octylthiophene) (P3OT). The d spacings and the volumes of the orthorhombic and of the monoclinic unit cells are closely similar, since they correspond in essence to a different indexing of the same reciprocal lattice. Larger, high symmetry unit cells of the kind found for form I′ P3BT, involving a doubling of the layer axes a were also taken into consideration. Since they were eventually discarded, the corresponding indexing is not reported in Table 2.

The volume of the smaller unit cells is about 710 Å^3 and, with 4 monomer units corresponding to 2 chains, it implies a density of about 1.30 g cm^{-3}, which is clearly higher than the value of 1.24 g cm^{-3} determined for form I′ P3BT.[24] This density value, which is applicable to all the mentioned P3BT form II lattices, appears qualitatively consistent with the greater thermodynamic stability of form II at room temperature. The idea that form II is the more stable form is discussed in some detail for P3BT in ref 14, although some speculations on the issue were formulated earlier as a general case for P3AT's.[15]

Molecular models of a regioregular and thus directional P3AT chain complying with the equivalence postulate of monomer units[25] may either display 2-fold screw symmetry ($p112_1$ rod group),[32] or glide symmetry, with a glide plane parallel to the chain axis b ($p\ b11$ rod group). If both symmetry elements are present, a fully planar chain with $p\ mb2_1$ rod group symmetry[32] will result, with the insurgence

of the plane of symmetry coinciding with the plane containing both the main chain and the side chains. This simple analysis applies if we disregard the possibility of disorder. Under the latter hypothesis, also the 2_1 symmetry implies a nearly planar conformation for P3AT chains. As to a possible intramolecular glide plane, if it is to be crystallographic, it must be orthogonal to one of the lattice vectors of an orthorhombic unit cell, or to the unique axis of a monoclinic one. Furthermore, to achieve reasonable main chain stacking, intramolecular crystallographic glide planes require a nearly zero value of the setting angle for planar P3AT chains (i.e., the angle between the main chain plane and the plane orthogonal to the stacking axis). This requirement constrains possible packings in ways that appear hardly reasonable, considering the value of the stacking axis (9.40 Å). We will not pursue this discussion further since subsequent refinements indicate that the 2_1 helical conformation is adopted in form II P3BT, in analogy to what found in form I′ P3BT.

Efficient intralayer stacking of main chains is a feature common to all previous detailed structural investigations of P3AT systems.[20−24] As previously discussed,[20b,24] starting from 2_1 helical main chain conformations, this packing may be attained crystallographically only with two symmetry operations, namely the inversion center *i* and the 2-fold rotation axis parallel to the main chain (see ref 24, Figure 5). Aside from chirality issues, the main difference between the two operations involves the relative orientation of the main chains in a stack. The inversion center *i* produces chains of opposite directionality (alternating up−down chains), while the 2-fold rotation axis produces chains with the same directionality. The latter was found in the case of the form I′ P3BT[24] and of the poly(3-(*S*)-2-methylbutylthiophene) (P3MBT)[20b] crystal structures.

We may note at this point that, since the stack is the fundamental supermolecular module in P3AT crystals, it is reasonable to expect a different intrastack symmetry for different polymorphs of the same polymer, especially if the chain conformation is preserved. Given the substantial differences between the form I and the form II structural families, plausibly involving different degrees of interdigitation and setting angles, the most likely intrastack operation for form II is not the 2-fold axis but rather the inversion center.

The next step in the analysis involves identifying the symmetry operations which give rise to the crystallographic interlayer periodicity and complete the space group symmetry. The plausible symmetry operations are the simple translational symmetry, which for molecules with 2_1 helical symmetry corresponds to a 2_1 packing symmetry operator parallel to the chain axis, or else 2-fold screw axis 2_1 perpendicular to the main chain axis, the inversion center and various types of glide planes perpendicular or parallel to the main chain axis. The analysis corresponds roughly to that carried out for the form I′ structure of P3BT[24] and the more plausible space groups are the same, namely $C222_1$, $P2_1/c$, $C2/c$, $Pca2_1$, and *Pbca*. All of these allow the presence in the crystal of antiparallel chains, at variance with otherwise acceptable space groups like *C*2, *Pc*, and $P2_1$, which imply chains with identical orientations. Because of this unphysical feature, the latter were not considered further.

The electron diffraction patterns[14b] suggests systematic absences for *h*0*l* reflections with *l* odd and 0*k*0 reflections with *k* odd if we adopt either of the two lattices in Table 2. These systematic absences, together with the intramolecular and packing symmetry considerations just discussed, are very hard to reconcile with any orthorhombic space group: indeed they point very strongly to two monoclinic space groups. The foremost is $P2_1/c$ with chains axes coinciding with the screw axes, and the inversion center as intrastack symmetry operator. The most significant alternative possibility is the $C2/c$ space group, which requires doubling of the *a* axis in the cells given in Table 2. We note that these two space groups are among the most frequent in nonchiral crystal structures of organic molecules, whereas $C222_1$ seems highly unlikely because it would imply that different polymorphs of the same polymer adopt a different lattice but identical space group.

Structural Refinement Based on X-ray Diffraction Data. A number of models were explored, in both the $P2_1/c$ and the $C2/c$ space groups. Only interdigitated side chain models gave encouraging results. The crystal structure of form II P3BT was refined using the Rietveld technique,[33] i.e., by the best fitting of the whole X-ray powder pattern profile. The program "Debvin",[34] which allows constrained refinements using large amounts of available a priori structural information, was used throughout. Sets of data from all the three different samples were used for the refinement. Both chain models with the side-chains coplanar (CPS) and at about 90° (OPS) with respect to the main chain were explored. CPS models with the side-chain coplanar to the main chain were initially promising and gave relatively good disagreement factors at low angles. However a splitting of the maximum at $2\theta \approx 20°$ arose and the R_2' disagreement factor ($R_2' = \Sigma|I_{obs} - I_{calc}|/\Sigma I_{net}$ where $I_{net} = I_{obs} - I_{bkg}$) is typically 20−30% higher than in the case of OPS models. Attempts to reduce the disagreement factor adopting CPS models lead to inappropriately distorted main chain models.

Using the best $P2_1/c$ OPS model, the lattice parameters refined to the following values, which are the result of an averaging of the results over the refinements with data sets from all three samples: $a = 10.76(1)$ Å, $b = 7.77$ (2) Å, $c = 9.44(2)$ Å, and $\beta = 64.66°$ ($V = 713.30$ Å^3), yielding a calculated density of 1.287 g/cm^3. The internal coordinates for P3BT form II are listed in Table 3 (see Figure 3 for the atomic labeling), while the final fractional atomic coordinates of all non-hydrogen atoms are reported in Table 4. The observed and calculated profiles are reported in Figure 4 together with the amorphous curve used in the fitting. Views of the refined molecular conformation and of the packing are shown in Figure 5. The final disagreement factor is $R_2' = 0.083$, using the data set obtained from the higher molecular weight AG fraction. Slightly higher values were obtained with data from the other samples. The fit is reasonably satisfactory also in the 2θ region between 35° and 45°. The overall stereochemistry appears acceptable: the shortest contact involving non-hydrogen atoms is between the S atoms of adjacent chains related by a center of symmetry (S1···S1′ 3.76 Å) within a stack. The shortest contacts between carbon atoms also occur within individual stacks

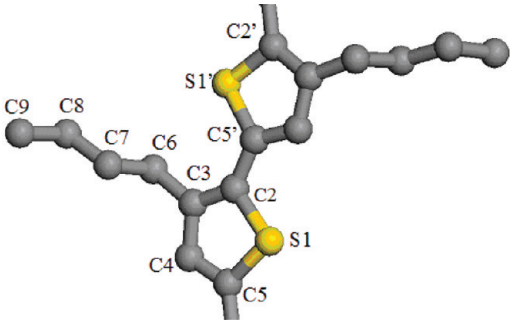

Figure 3. Chain model with atomic numbering scheme.

Table 3. Refined Internal Coordinates for Poly(3-butylthiophene), Form II[a]

Bond Lengths (Å)			
C5−S1	1.735[b]	C2−S1	1.737[b]
C2−C3	1.375[b]	C4−C5	1.365[b]
C3−C4	1.424	C3−C6	1.510[b]
C5−C2′	1.430	C6−C7	1.530[b]
C7−C8	1.530[b]	C8−C9	1.530[b]
Bond Angles (deg)			
C5−S1−C2	93.0[b]	S1−C2−C3	110.2[b]
S1−C5−C4	109.7[b]	C5−C4−C3	114.4
C2−C3−C6	126.6	C2−C3−C4	112.7
C4 −C3−C6	120.7	C3−C6−C7	110.4
C2′−C5−S1	122.9	C6−C7−C8	109.9
C5 −C2′−S1′	117.3	C7−C8−C9	109.9
C2′−C5−C4	127.3	C3−C2−C5′	132.4
Torsion Angles (deg)			
S1−C5−C4−C3	0.0	C2−C3−C4−C5	0.0
C2−C3−C6−C7	−96.9	C3−C6−C7−C8	−175.4
C4−C3−C6−C7	83.3	C6−C7−C8−C9	175.3
S1−C2−C3−C6	180.2	S1′−C2′−C5−S1	176.0
C5−C4−C3−C6	179.8	S1′−C2′−C5−C4	−1.5
C3′−C2′−C5−C4	−177.3	C5′−S1′−C2′−C5	−176.7
C3′−C2′−C5−S1	0.1	C2′−C5−C4−C3	177.7

[a] Estimated standard deviations vary between 0.3 and 1.0° for bond angles, and between 1.0 and 2.0° for torsion angles. [b] Values not refined.

Table 4. Refined Atomic Parameters of Non-Hydrogen Atoms in Poly(3-butylthiophene) Form II

	X	*Y*	*Z*	*B* (Å^2)
C2	0.0246(5)	0.3165(17)	0.2248(3)	3.9
C3	0.1194(6)	0.3943(17)	0.0915(3)	3.9
C4	0.1087(8)	0.5770 (17)	0.0976(3)	3.9
C5	0.0077 (9)	0.6400(17)	0.2329(3)	3.9
C6	0.2260(9)	0.3052(19)	−0.0509(6)	3.9
C7	0.3646(8)	0.3008(27)	−0.0420 (16)	3.9
C8	0.4743(12)	0.2234(35)	−0.1927(22)	3.9
C9	0.6151(11)	0.2324 (50)	−0.1896(34)	3.9
S1	−0.0769(7)	0.4709(17)	0.3567(4)	3.9

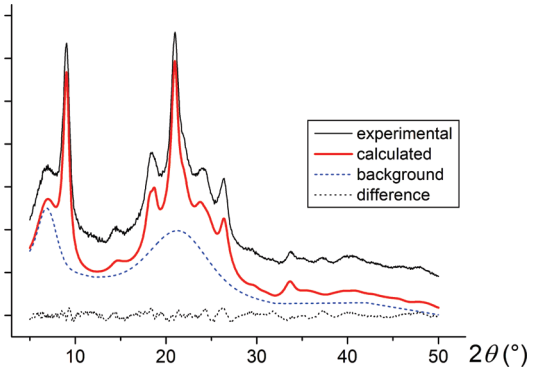

Figure 4. The upper curve is the experimental unoriented X-ray diffraction pattern of form II poly(3-*n*-butylthiophene) obtained from the AG sample while the calculated pattern is the thicker red line (experimental curve arbitrarily displaced vertically to facilitate visual comparison). The dashed blue line is the amorphous and background contribution adopted to optimize the fit. The difference curve (dotted) between the experimental and the calculated pattern is shown at the bottom.

and measure 3.87 Å (between two sp^2 carbons) and 3.95 Å (between two sp^3 carbons). As to the interdigitated side chains of adjacent stacks, the shortest contact occurs between C8 atoms related by a 2_1 axis and measures 4.01 Å. The

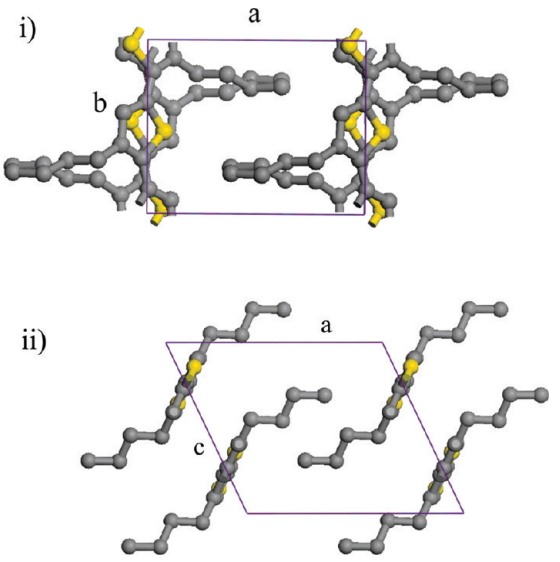

Figure 5. (i) Crystal structure of poly(3-butylthiophene) form II viewed laterally along the stacking axis **c** and (*ii*)molecular packing viewed down the **b** axis (only non-hydrogen atoms are shown in this case).

Table 5. Form II P3BT Crystal Structure Models in Space Group $P2_1/c$ Obtained by Rietveld Refinement and Their Energy in kcal/mol of Chemical Repeat Units (c.r.u.'s) from Subsequent Molecular Mechanics Minimizations[a]

Form II, $P2_1/c$, Out-of-Plane Side Chains (OPS Model)	
diffraction experimental	MM minimization
a = 10.76 Å	10.71(−0.46%)
b = 7.77 Å	7.81 (+0.51%)
c = 9.44 Å	8.92 (−5.51%)
β = 64.66°	69.45°
V_{CR}[b] = 178.33 Å^3	V_{CR}[b] = 174.66 Å^3
density = 1.29 g/cm^3	1.32 g/cm^3 (+2.2%)
C2−C3−C6−C7 torsion angles: ± 97.1°	±95°
potential energy per cru (kcal/mol)	−14.88 (−13.98)[c]
Form II, $P2_1/c$, In-Plane Side Chains (CPS Model)	
diffraction experimental	MM minimization
a = 10.77 Å	10.71(−0.60%)
b = 7.80 Å	7.83 (+0.38%)
c = 9.34 Å	9.09 (−2.68%)
β = 63.94°	β = 63.59°
V_{CR}[b] = 176.21 Å^3	V_{CR}[b] = 170.68 Å^3
density = 1.31 g/cm^3	1.35 g/cm^3 (+2.9%)
C2−C3−C6−C7 torsion angles: ± 174.7°	±178°
potential energy per cru (kcal/mol)	−14.20 (−13.93)[c]
Form I′, $C222_1$ Space Group[24]	
diffraction experimental	MM minimization
V_{CR}[b] = 184.81 Å^3	V_{CR}[b] = 187.88 Å^3
density = 1.24 g/cm^3	1.22 g/cm^3 (−1.7%)
potential energy per cru (kcal/mol)	−12.98 (−12.88)[c]

[a] Form I′ P3BT[24] energy and density data obtained with the same force field data are also given for comparison. All data were obtained with force field FF3 from ref 26e. [b] Volume per cru (chemical repeat unit). [c] Minimization with fixed experimental lattice parameters.

chain setting angle, defined as the angle between the least-squares planes of the P3BT main chains and the lattice planes perpendicular to **c***, i.e. the [00*l*] planes, measures about 65°. This feature appears to be different from the proposed models of form II structures of poly(3-octylthiophene) (P3OT) and poly(3-dodeylthiophene) (P3DDT),[15] while it agrees qualitatively with other literature suggestions.[17] Indeed the stacking in individual layers resembles somewhat that

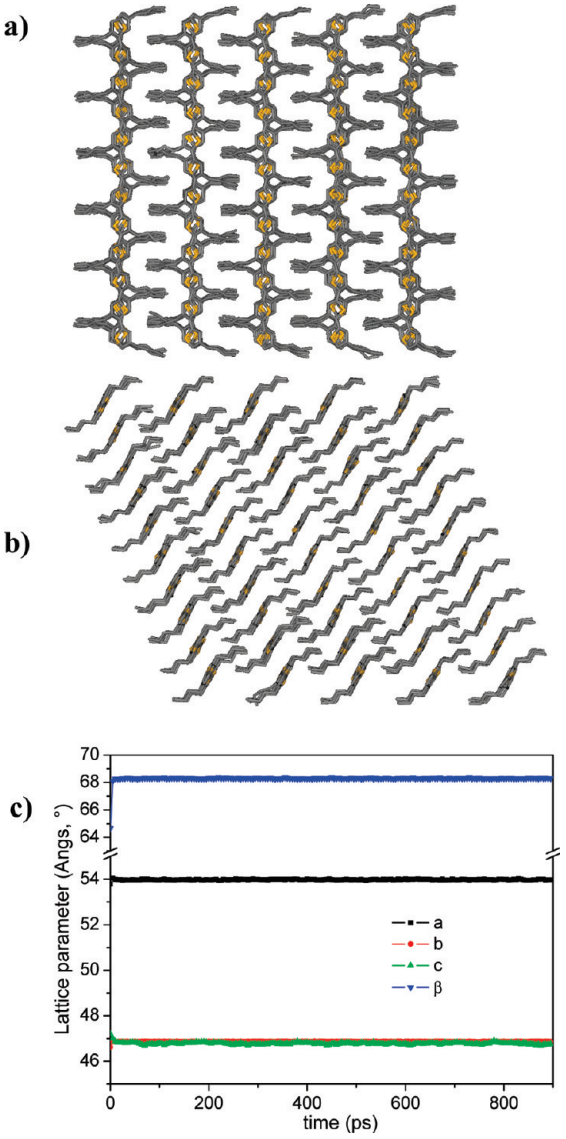

Figure 6. MD results for the OPS P3BT form II $P2_1/c$ model after 900 ps at 300 K and 1 bar: (a) view along the **c** lattice direction, (b) along the **b** direction, and (c) lattice parameters evolution.

found in polythiophene,[35] with the axial shift between adjacent chains resulting from a compromise between efficient packing of alkyl side chains (see Figure 5), and efficient stacking of thiophene rings[36] of adjacent main chains.

Molecular and Crystal Modeling. The most promising models obtained by refinement of the diffraction data were also examined by MM minimization of their potential energy. Minimizations were always performed starting with molecules in 2_1 helical conformations, either with coplanar side chains or with side chains roughly orthogonal to the main chain (CPS and OPS models, corresponding to $p112_1$ and $pmb2_1$ rod group symmetries[32]). The crystal symmetry was used in the construction of the models, but it was not enforced in the MM minimizations. In a first cycle of calculations the energy of a crystal polymorph was minimized with respect to the atomic coordinates only. The lattice parameters were then allowed to vary in a second set of calculations. MD simulations were finally carried out for the most significant models, to check the stability of the minimized structures. The results to be presented below were obtained with the same version of our force-field (FF3 in

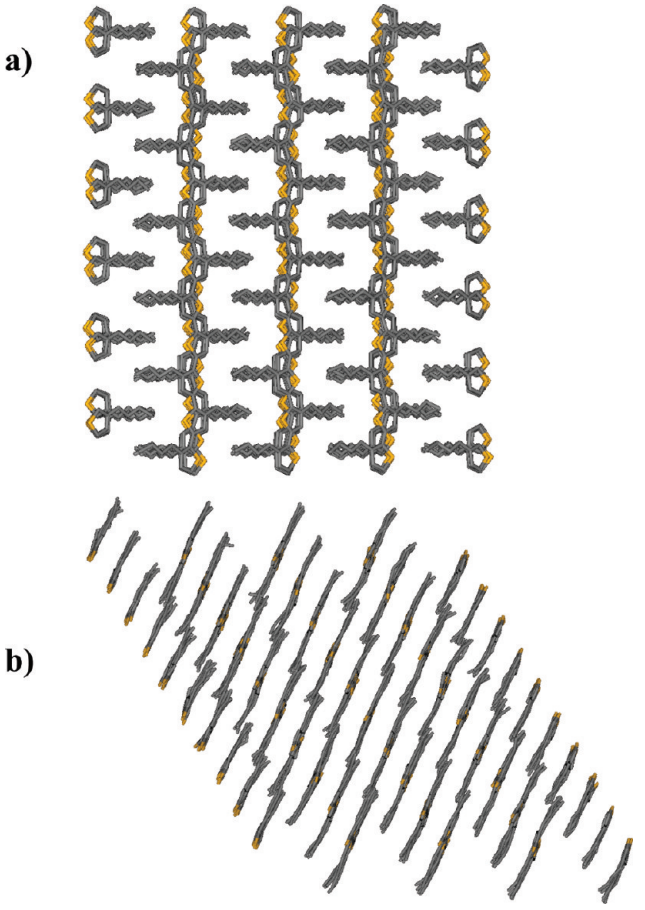

Figure 7. MD results for the CPS P3BT form II $P2_1/c$ model after 300 ps at 300 K and 1 bar: (a) view along the **c** lattice direction; (b) along the **b** direction;.

ref 26e), but qualitatively similar results were obtained also with earlier versions.

Both the $C2/c$ and the $P2_1/c$ space group were initially investigated. In the former case, the refinement produced results with relatively low energies but involving major structural alterations, which made them incompatible with the X-ray diffraction data. We will therefore concentrate our discussion on the results obtained with space group $P2_1/c$, which are summarized in Table 5.

The lattice parameters and chain conformation (in particular the C2-C3-C6-C7 torsion angle connecting the side-chain to the backbone) stay close to their original values in the $P2_1/c$ structures with both the CPS and the OPS models, converging to well-defined minimum-energy structures. Compared to the form I′ structure, both of these minima have a higher density and are more stable by 1−2 kcal/(mole of c.r.u.). Somewhat surprisingly, the planar CPS model has higher density but also slightly higher potential energy than the OPS model.

MD simulations give additional insights into the structural organization of form II P3BT. The simulations were carried out using a $5 \times 6 \times 5$ supercell in which the a, b, c lattice parameters were allowed to vary freely along with the angle β, whereas the α and γ angles are kept at 90°. Under room T and P conditions (300 K and 1 bar, respectively), the OPS model of form II is extremely stable. The lattice lengths remain in essence very close to their experimental values, whereas β expands by 3.5° from the experimental, to adopt the average value of 68.2°. The structure shown in Figure 6 remains highly ordered. The side chain conformations

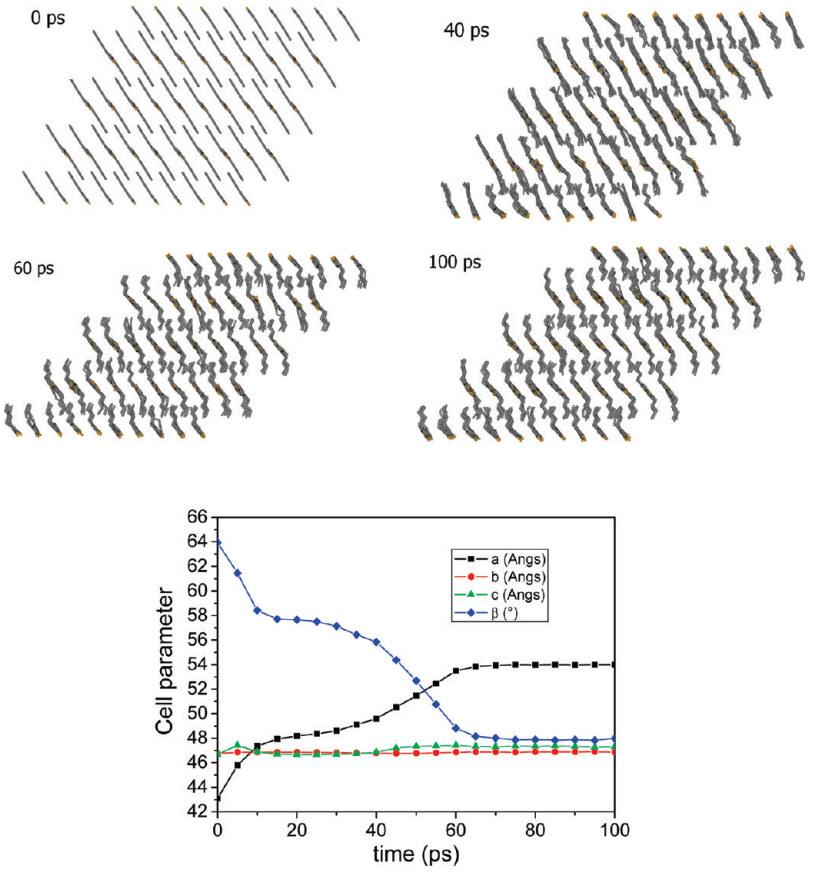

Figure 8. MD results for the CPS P3BT form II $P2_1/c$ model, viewed along the **b** direction at 340 K and 1 bar after the indicated time evolution (ps). The graph shows the evolution of the lattice parameters.

Table 6. Disagreement Factor, Refined Crystallite Dimensions (Coherence Lengths), and Estimated Form II Crystallinity for the Three Studied Samples

sample	R_2'	$l_b(ch.ax)$ (Å)	$l_c(rad)$ (Å)	l_a (Å)	x_{crys} FII
S	0.118	25	190	60	~50
AD	0.102	20	160	70	~55
AG	0.083	20	370	40	~42

and their correlation are largely maintained, along with the overall 2_1 helical molecular conformation.

The MD behavior of the planar CPS $P2_1/c$ model is remarkably different: the structure is initially metastable, after a contraction of the β angle from 64° to about 58° (Figure 7). However after a variable time, depending upon minor force-field details[26] and the temperature value, the structure irreversibly evolves to the nonplanar OPS structure. Figure 8 displays the key steps and features of this transformation as it occurs at 340 K (i.e., above room temperature but well below the experimental melting temperature of form II, which occurs around 430 K[14b]), adopting the force field version for which all the energy values in this paper were obtained. It can be seen that at 40 ps, around the beginning of the transformation leading to the final crystal structure, there are a few orthogonal side chains coexisting with a majority of coplanar ones. These orthogonal butyls seem to act as nucleation sites for the transformation to the new OPS structure, which appears to be almost complete within the subsequent 20 ps. The MD behavior of the CPS structure is remarkably consistent with the diffraction refinement results, which clearly favor the OPS model over the CPS structure. We may on the other hand speculate that at high pressure and at low enough temperatures the CPS structure may become the more stable structure because of its remarkably higher density.

Morphological Implications of the Structural Refinement. Table 6 summarizes the coherence lengths along the three lattice directions and the crystallinity of form II, determined from the Rietveld refinements using the data sets from the three investigated P3BT samples (see Figure 2; molecular weights and related data are in Table 1). The crystallinity in the higher molecular weight sample AG is significantly lower than in the lower molecular weight AD and S samples. This is a general trend in poly(3-alkylthiophenes), reflecting increasing obstacles to crystallization with increasing molecular mass.

A remarkable common result of the refinements with all three data sets is the extremely small coherence length l_b of 20−25 Å (i.e., about 6 monomer units) along the chain axis direction. The average fully extended chain length is at least 6 times l_b in the case of the lower molecular weigh sample AD, and up to ca. 40 times that value for the AG sample, even assuming that polystyrene-equivalent MW are overestimated by about 40%.[37] To achieve the crystallinity values we determined it is nearly mandatory to postulate chain folding, given the small value of coherence length in the axial direction. A chain folded lamellar structure is also made very plausible by the spherulitic morphology described in the literature and apparent also in our samples (Figure 1). The fact that the crystalline stem length refines to ca. 6 monomer units and that the same number of thiophene units are required for tight folds can easily be reconciled with the crystallinity values of about 50% (see Table 6) assuming that the low molecular weight S and AD sample essentially consist of chain folded crystals with a thickness of about

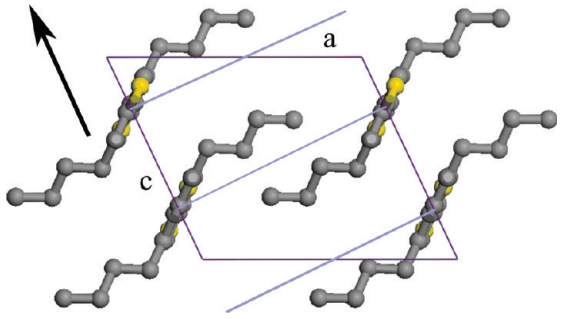

Figure 9. Form II P3BT crystal structure viewed down the **b** axis. Relevant [204] planes connecting chain stems separated by 9.7 Å and with opposite orientation are evidenced in blue. The black arrow parallel to **c** indicates the [204] or the equivalent [102] radial direction in form II P3BT spherulites. The main chain lie in planes nearly parallel to the [101] plane.

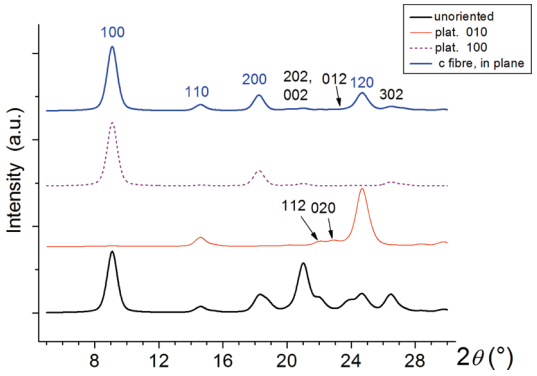

Figure 10. Diffraction patterns calculated from the OPS P3BT form II $P2_1/c$ refined model for a fully crystalline sample in Bragg−Brentano geometry adopting a peak width similar to the experimental value. The thick black profile results assuming absence of preferred orientation. Fiber or needle crystals with principal axis in the plane of the sample film corresponding to the *c* crystal axis, i.e., assuming that this axis corresponds to the spherulite radius, give the thick blue line diffraction pattern. The thin black line and the dotted line patterns are obtained respectively from flat on lamellae with the normal to the lamellar surface corresponding respectively to the **b***, i.e., the **b** axis direction and the **a*** lattice direction.

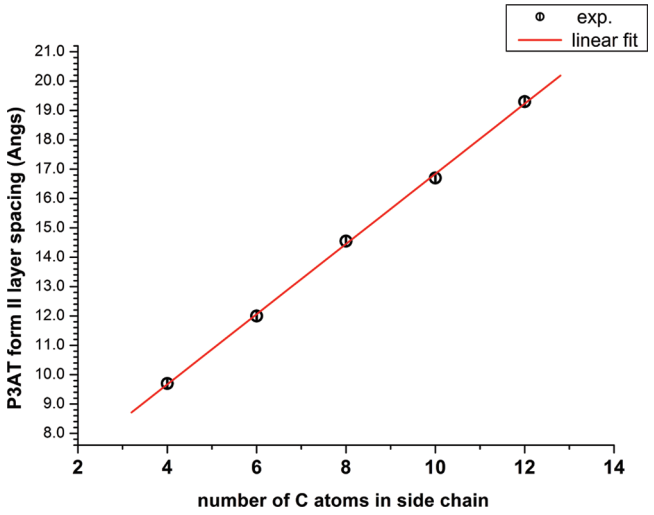

Figure 11. Regioregular P3AT form II layer spacing as a function of the side chain carbon number. The clear linear dependence suggests a unique, well-defined structural family. The data for P3BT are from the present work, for P3HT from ref 18, for P3OT and P3DDT from ref 15, and for poly(3-decylthiophene) (P3DT) from refs 16a and 17.

40 Å. In the case of the higher molecular weight AG sample the lower crystallinity requires the presence of a significant amorphous component beyond chain folds.

As apparent from the published electron diffraction patterns (see Figure 7d in ref 14, the **c** axis, obviously orthogonal to the **a*** and the **b*** reciprocal axes, coincides with the radial direction of the spherulites, which clearly is the fast growth direction of form II P3BT crystals. It is remarkable that the **c** direction corresponds to the axis along which the stacking of the polythiophene main chains occurs (Figure 5, and, according to the refinement, it is also the direction along which form II crystals have relatively large coherence lengths (> 150 Å). Note that, whereas the [001] planes contain chains stems all sharing the same orientation, the [102] or better the [204] planes (see Figure 9) which are nearly orthogonal (at 89.4°) to the fast growth direction, i.e., the **c** axis, contain antidirectional chain stems, related by a center of symmetry at the center of the unit cell and separated by ∼9.7 Å. This amounts to almost ideal conditions for chain folding, through loops in which 5 thiophene units are connected by cisoid conformations[38] (see also Figure 8 of ref 24). The [204] planes thus represent nearly ideal fold planes on the basis of our crystal structure model. On the contrary, the [100] planes which also contain antidirectional chains separated a distance of 4.7 Å, are for this short distance quite unlikely to represent fold planes.

The refined crystal structure model also allows to determine the preferred orientation in spherulitic thin films of P3BT: while the diffraction patterns in Figure 2 correspond in essence to random crystallite orientations (compare to Figure 10, thick black line), the form II P3BT diffraction patterns in the literature (see for example Figure 2 and Figure 6, profile b, of ref 14), are evidently patterns from oriented specimens. The calculated diffraction patterns from different modes of orientation[39] are compared in Figure 10. The results rule out that thin films patterns are due to lamellar single crystals with the chain axis (i.e., **b** according to our indexing) orthogonal to flat-on lamellae, as suggested in recent work.[14] If that were the case, the strong 120 reflection at $2\theta = 24.7°$ would dominate the pattern, since the 020 reflection at $2\theta = 22.9°$ is weak (see thin red profile in Figure 10). The diffraction patterns by thin form II P3BT films in the literature (Figure 2 and Figure 6, profile b of ref 14 and the related electron diffraction patterns) can be interpreted in terms of needle-like, or fiber crystals with the principal axis, i.e. the form II spherulite radius, coinciding with the stacking axis **c**, lying in the plane of the film, while **a** and **b** (chain axis) are randomly oriented around it (see thick blue profile in Figure 10). The correct indexing of the patterns, also shown in Figure 10, supports this interpretation, which appears persuasive considering that the typical film thicknesses (10−20 nm), for both our film samples and in ref 14, is smaller by a factor of $\sim 10^2$ than the average spherulite radius (around 10 μm). Substantially thicker spherulitic films were not investigated, but should present a significant reduction of the in-plane orientation of the stacking axis **c**.

Yang and collaborators have on the other hand convincingly shown (Figure 10, parts b and c, of ref 14b that, upon annealing, form II spherulites transform to form I maintaining the spherulitic morphology at temperatures ca. 100 °C below the final form I melting point. As the authors state, electron diffraction patterns (Figure 10c of ref 14b) indicate that in the transformation the preferred orientation of the stacking direction along the radial spherulitic direction is indeed maintained also in form I. However also in this case

both the pattern and the morphology should plausibly be interpreted assuming a random, fiber-like orientation of the chain axis (and the long lamellar axis) around the radial direction. It appears that the lamellae in form II spherulites, which evolve to form I after appropriate annealing, are related to the whisker or nanowire[10c,13,40] form I morphology obtained with various P3AT's from concentrated solutions.

Conclusions

The structure of form II P3BT was determined and refined by Rietveld analysis. It has also been confirmed by molecular mechanics (MM) and molecular dynamics calculations adopting a thiophene-specific force field. Consistent with its higher density, and with thermal data that indicate that form II is the thermodynamically stable structure at low temperatures, it shows lower potential energy than the form I′ crystalline polymorph of P3BT. Both the main-chain and the side chain conformation is the same as proposed for the form I′ polymorph. The form II refined structural model however presents a looser, tilted, antidirectional stacking and tightly interdigitated layering, different from those observed in the form I family of poly(3-alkythiophenes) (P3AT's). Our model is broadly consistent with proposals by Winokur et al.[15] for the structures of highly regioregular form II P3OT and P3DDT but substantially more detailed. It is also consistent with ^{13}C MAS NMR data pertaining to form II P3OT, which indicates that the crystalline main chains adopt in this polymorph a rigorously transplanar main chain conformation.[16b] The strictly linear correlation between the form II lamellar spacing of P3AT's with different side chain length (Figure 11) is strongly suggestive of the fact that the detailed form II structural model developed for P3BT essentially applies also to higher P3AT's with longer side chains.

The 20−25 Å crystallite dimension along the chain axis direction, and the lamellar structure typical of spherulitic morphology of form II P3BT imply substantial chain-folding, consistent with the fact that form II polymorphs in P3ATs are obtained by crystallization in the presence of solvent. Oriented diffraction patterns from thin films of form II P3BT are explained on the basis of the proposed crystal structure assuming that the stacking axis (i.e., **c** according to our indexing), corresponding to the fast growth direction and to the radius of the bidimensional form II spherulites, is preferentially in the plane of the film, while the layer axis a and the chain axis c approach random orientation rather at variance with suggestions in recent publications.

Form II of P3BT and plausibly of the other P3AT's[15,16] appear to be more stable and more ordered[16b] than the form I family. Our investigation confirms that in crystals of this polymorph there is a high degree of main chain planarity, which MD calculations still in progress imply that is maintained also above room temperature. These features are consistent with the higher density of this polymorph and may suggest to a superficial observer that form II is ideally suited for organic electronic applications. However, the very small crystal dimensions in the chain-axis direction, the less compact stacking and the plausible relevance of widespread chain folding could well be factors making this modification more prone to charge trapping. These features, along film discontinuity implied by the relatively high crystallinity and the spherulitic morphology, suggest in fact limitations to charge mobility except possibly in the stacking direction, in which coherence lengths are remarkable (20−40 nm for P3BT). These observations may explain why form II is less attractive than the annealed form I polymorph family for molecular electronics and, to our knowledge, it has never been identified in any of the P3AT of the more efficient active layers of electronic devices. It appears that the molecular weights and the processing conditions used to optimize the performance of active P3AT layers[2,9,41] in essence preclude the presence of the form II polymorphs in the active layers of devices with optimum performance. In this context we remark that, for reasons that are still not fully understood, the most widely used P3AT, namely P3HT appears to be particularly defiant to crystallization in form II. In the two cases[18] where clear evidence of form II P3HT crystallization are given, it occurs only for molecular masses of 2−3 kDa and along with predominant form I .

Acknowledgment. Funding by ENI SpA, also involving support to A.B., is gratefully acknowledged.

Supporting Information Available: Table of refined nonstructural parameters along with text dicussing the details of the structural refinement procedure. This material is available free of charge via the Internet at http://pubs.acs.org.

Note Added after ASAP Publication. This article posted ASAP on July 22, 2010. The title of the paper has been revised. The correct version posted on July 28, 2010.

References and Notes

(1) (a) Yu, G.; Gao, J.; Hummelen, J. C.; Wudl, F.; Hegeer, A. J. *Science* **1995**, *270*, 1789. (b) Hegeer, A. J. *Angew. Chem., Int. Ed.* **2001**, *40*, 2591.
(2) Thompson, B. C.; Fréchet, J.-M. *Angew. Chem., Int. Ed.* **2008**, *47*, 58.
(3) Kline, R. J.; McGeHee, M. D. *J. Macromol. Sci., C, Polym. Rev.* **2006**, *46*, 27.
(4) Sirringhaus, H. *Adv. Mater.* **2005**, *17*, 2411.
(5) Barbour, L. W.; Hegadorn, M.; Asbury, J. B. *J. Am. Chem. Soc.* **2007**, *129*, 15884.
(6) (a) Bredas, J. L.; Beljonne, D.; Coropceanu, V.; Cornil, L. *Chem. Rev.* **2004**, *104*, 4971. (b) Bredas, J. L.; Norton, E. J.; Cornil, L.; Coropceanu, V. *Acc. Chem. Res.* **2009**, *42*, 1691.
(7) Cheung, D. L.; McMahon, D. P.; Troisi, A. *J. Am. Chem. Soc.* **2009**, *131*, 11179.
(8) Kaake, L. G.; Barbara, P. F.; Zhu, X.-Y. *J. Phys. Chem. Lett.* **2010**, *1*, 628.
(9) (a) Günes, S.; Neugebauer, H.; Sariciftci, N. S. *Chem. Rev.* **2007**, *107*, 1324. (b) Po, R.; Maggini, M.; Camaioni, N. *J. Phys. Chem. C* **2010**, *114*, 695. (c) Hains, A. W.; Liang, Z.; Woodouse, M. A.; Gregg, B. A. *Chem. Rev.*, **2010**, in press.
(10) (a) Bao, Z.; Dodabalapur, A.; Lovinger, A. J. *Appl. Phys. Lett.* **1996**, *69*, 4108. (b) Garnier, F. Field-Effect Transistors Based on Conjugated Materials. In *Electronic Materials: The Oligomer Approach*; Müllen, K., Wegner, G., Eds.; Wiley-VCH: Weinheim, Germany, 1998; (c) Zhang, R.; Li, B.; Iovu, M. C.; Jeffries-EL, M.; Sauvé, G.; Cooper, J.; Jia, S.; Tristram-Nagle, S.; Smilgies, D. M.; Lambeth, D. N.; McCullough, R. D.; Kowalewski, T. *J. Am. Chem. Soc.* **2006**, *128*, 3480.
(11) (a) Kraft, A.; Grimsdale, A. C.; Holmes, A. B. *Angew. Chem., Int. Ed.* **1998**, *37*, 402. (b) Köhler, A.; Wilson, J. S.; Friend, R. H. *Adv. Mater.* **2002**, *14*, 701. (c) Perepichka, I. F.; Perepichka, D.; Meung, H.; Wudl, F. *Adv. Mater.* **2005**, *17*, 2281.
(12) (a) Kim, J. Y.; Lee, K.; Coates, N. E.; Moses, D.; Nguyen, T.-Q.; Dante, M.; Heeger, A. J. *Science* **2007**, *317*, 222. (b) Osaka, I.; McCullough, R. D. *Acc. Chem. Res.* **2008**, *41*, 1202. (c) *Handbook of Thiophene-Based Materials*; Perepichka, I. F., Perepichka, D. F., Eds.; Wiley-Blackwell: Chichester, U.K., 2009; Vols. *1* and *2*.
(13) (a) Xin, H.; Kim, F. S.; Jenekhe, S. A. *J. Am. Chem. Soc.* **2008**, *130*, 5424. (b) Xin, H.; Ren, G.; Kim, F. S.; Jenekhe, S. A. *Chem. Mater.* **2008**, *20*, 6199.
(14) (a) Lu, G. H.; Li, L. G.; Yang, X. N. *Adv. Mater.* **2007**, *19*, 3594. (b) Lu, G. H.; Li, L. G.; Yang, X. N. *Macromolecules* **2008**, *41*, 2062.
(15) Prosa, T. J.; Winokur, M. J.; McCullough, R. D. *Macromolecules* **1996**, *29*, 3654.
(16) (a) Bolognesi, A.; Porzio, W.; Provasoli, F.; Ezquerra, T. *Makromol. Chem.* **1993**, *194*, 817. (b) Bolognesi, A.; Porzio, W.; Provasoli, A.; Comotti, A.; Sozzani, P.; Simonutti, R. *Makromol. Chem. Phys.* **2001**, *202*, 2586.
(17) Meille, S. V.; Romita, V.; Caronna, T.; Lovinger, A. J.; Catellani, M.; Belobrzeckaja, L. *Macromolecules* **1997**, *30*, 7898.
(18) (a) Zen, A.; Saphiannikova, M.; Neher, D.; Grenzer, J.; Grigorian, S.; Pietsch, U.; Asawapirom, U.; Janietz, S.; Scherf, U.; Lieberwith,

I.; Wegner, G. *Macromolecules* **2006**, *39*, 2162. (b) Joshi, S.; Grigorian, S.; Pietsh, U. *Phys. Status Solidi A* **2008**, *205*, 488.
(19) (a) Brinkmann, M.; Rannou, P. *Adv. Func. Mater.* **2007**, *17*, 101. (b) Brinkmann, M.; Rannou, P. *Macromolecules* **2009**, *42*, 1125.
(20) (a) Catellani, M.; Luzzati, S.; Bertini, F.; Bolognesi, A.; Lebon, F.; Longhi, G.; Abbate, S.; Famulari, A.; Meille, S. V. *Chem. Mater.* **2002**, *14*, 4819. (b) Arosio, P.; Famulari, A.; Catellani, M.; Luzzati, S.; Torsi, L.; Meille, S. V. *Macromolecules* **2007**, *40*, 3.
(21) (a) Winokur, M. J.; Wamsely, P.; Moulton, J.; Smith, P.; Heeger, A. J. *Macromolecules* **1991**, *24*, 3812. (b) Prosa, T. J.; Winokur, M. J.; Moulton, J.; Smith, P.; Heeger, A. J. *Macromolecules* **1992**, *25*, 4364.
(22) (a) Tashiro, K.; Ono, K.; Minagawa, Y.; Kobayashi, M.; Kawai, T.; Yoshino, K. *J. Polym. Sc. Part B, Polym Phys.* **1991**, *29*, 1223. (b) Tashiro, K.; Kobayashi, M.; Kawai, T.; Yoshino, K. *Polymer* **1997**, *38*, 2867.
(23) (a) Mardalen, J.; Samuelsen, E. J.; Gautun, O. R.; Carsen, P. H. *Solid State Commun.* **1991**, *77*, 337. (b) Mardalen, J.; Samuelsen, E. J.; Gautun, O. R.; Carsen, P. H. *Synth. Met.* **1992**, *48*, 363.
(24) Arosio, P.; Moreno, M.; Famulari, A.; Raos, G.; Catellani, M.; Meille, S. V. *Chem. Mater.* **2009**, *21*, 78.
(25) Corradini, P. Chain Conformation and Crystallinity. In *The Stereochemistry of Macromolecules*; Ketley, A. D., Ed.; M. Dekker: New York, 1968; Vol. *3*, p 1.
(26) (a) Raos, G.; Famulari, A.; Marcon, V. *Chem. Phys. Lett.* **2003**, *379*, 364. (b) Marcon, V.; Raos, G.; Allegra, G. *Macromol. Theory Simul.* **2004**, *13*, 497. (c) Marcon, V.; Raos, G. *J. Phys. Chem. B* **2004**, *108*, 18053. (d) Marcon, V.; Raos, G. *J. Am. Chem. Soc.* **2006**, *128*, 1408. (e) Moreno, M.; Casalegno, M.; Raos, G.; Meille, S. V.; Po, R. *J. Phys Chem. B* **2010**, *114*, 1591.
(27) (a) McCullough, R. D.; Lowe, R. D.; Jayaraman, M.; Anderson, D. L. J. *J. Org. Chem.* **1993**, *58*, 904. (b) Corina, M. I.; Sheina, E. E.; Gil, R. R.; McCullough, R. D. *Macromolecules* **2005**, *38*, 8649. (c) Miyakoshi, R.; Yokoyama, A.; Yokozawa, T. *J. Am. Chem. Soc.* **2005**, *127*, 17542.
(28) Ponder, J. W. *TINKER: Software Tools for Molecular Design*, 4.2 ed.; Washington University School of Medicine: Saint Louis, MO, 2004.
(29) Materials Studio and Discover are products of Accelrys Inc. (see www.accelrys.com).
(30) (a) Destri, S.; Ferro, D. R.; Khotina, I. A.; Porzio, W.; Farina, A. *Macromol. Chem. Phys.* **1998**, *199*, 1973. (b) Siegrist, T.; Kloc, C.; Laudise, R. A.; Katz, H. E.; Haddon, R. C. *Adv. Mater.* **1998**, *10*, 379.
(31) Jorgensen, W. L.; Maxwell, D. S.; Tirado-Rives, J. *J. Am. Chem. Soc.* **1996**, *118*, 11225.
(32) *International Tables For Crystallography*; Kopsky, V., Litvin, D. B. , Eds.; IUCR/Kluwer Academic Publ.: Dordrecht, The Netherlands, 2002; *Vol. E*.
(33) Rietveld, H. M. *Acta Crystallogr.* **1967**, *22*, 151.
(34) Bruckner, S.; Immirzi, A. *J. Appl. Crystallogr.* **1997**, *30*, 207.
(35) Bruckner, S.; Porzio, W. *Makromol. Chem.* **1988**, *189*, 961.
(36) Tsuzuki, S.; Honda, K.; Azumi, R. *J. Am. Chem. Soc.* **2002**, *124*, 12200.
(37) Liu, J.; Loewe, R. S.; McCullough, R. D. *Macromolecules* **1999**, *32*, 5777.
(38) Mena-Osteritz, E.; Meyer, A.; Langeveld-Voss, B. M. W.; Janssen, R. A. J.; Meijer, E. W.; Bäuerle, P. *Angew. Chem., Int. Ed.* **2000**, *39*, 2679.
(39) Toraya, H.; Marumo, F. *Mineralog. J.* **1981**, *10*, 211.
(40) (a) Ihn, K.; Moulton, J.; Smith, O. *J. Polym. Sci., Part B: Polym Phys.* **1993**, *31*, 735. (b) Malik, S.; Nandi, A. K. *J. Polym. Sci., Part B: Polym Phys.* **2002**, *40*, 2073. (c) Merlo, J. A.; Frisbie, C. D. *J. Polym. Sci., Part B: Polym Phys.* **2003**, *41*, 2674. (d) Berson, S.; De Bettignies, R.; Guillerez, S. *Adv. Funct. Mater.* **2007**, *17*, 1377. (e) Lu, G.; Tang, H.; Qu, Y.; Li, L.; Yang, X. *Macromolecules* **2007**, *40*, 6579.
(41) (a) Camaioni, N.; Garlaschelli, L.; Geri, A.; Maggini, M.; Possamai, G.; Ridolfi, G. *J.Mater. Chem.* **2002**, *12*, 2065. (b) Le Huong, N.; Hoppe, H.; Erb, T.; Günes, S.; Gosch, G.; Sariciftci, N. S. *Chem. Rev.* **2007**, *107*, 1324.